NANO LETTERS

pubs.acs.org/NanoLett Letter

Sizable Band Gap in Epitaxial Bilayer Graphene Induced by Silicene Intercalation

Hui Guo,[⊥] Ruizi Zhang,[⊥] Hang Li,[⊥] Xueyan Wang, Hongliang Lu, Kai Qian, Geng Li, Li Huang, Xiao Lin, Yu-Yang Zhang, Hong Ding, Shixuan Du,* Sokrates T. Pantelides, and Hong-Jun Gao*

Cite This: *Nano Lett.* 2020, 20, 2674−2680 Read Online

ACCESS | Metrics & More | Article Recommendations | Supporting Information

ABSTRACT: Opening a band gap in bilayer graphene (BLG) is of significance for potential applications in graphene-based electronic and photonic devices. Here, we report the generation of a sizable band gap in BLG by intercalating silicene between BLG and Ru substrate. We first grow high-quality Bernal-stacked BLG on Ru(0001) and then intercalate silicene to the interface between the BLG and Ru, which is confirmed by low-energy electron diffraction and scanning tunneling microscopy. Raman spectroscopy shows that the G and 2D peaks of the intercalated BLG are restored to the freestanding-BLG features. Angle-resolved photoelectron spectroscopy measurements show that a band gap of about 0.2 eV opens in the BLG. Density functional theory calculations indicate that the large-gap opening results from a cooperative contribution of the doping and rippling/strain in the BLG. This work provides insightful understanding on the mechanism of band gap opening in BLG and enhances the potential of graphene-based device development.

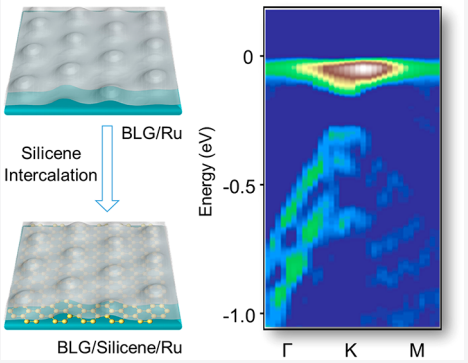

KEYWORDS: *bilayer graphene, band gap, cooperative mechanism, intercalation, silicene*

INTRODUCTION

Bilayer graphene (BLG) is an attractive material providing a fertile ground for fundamental studies of two-dimensional physics.[1,2] With different stacking configurations, many exotic phenomena such as tunable excitons,[3,4] topological valley transport,[5] Mott-like insulator states,[6] and superconductivity[7] have been discovered in BLG. Of particular interest, BLG in AB-stacking acquires an electronic band gap by breaking the inversion symmetry of the two layers, making it a promising high-mobility channel material that can be used in terahertz technology, nanoelectronic, and nanophotonic devices.[8−10]

Application of an external electric field[11−14] or adsorption of molecules/atoms on BLG surfaces,[15−19] which create a potential difference between the two graphene layers, are two experimentally proven strategies to introduce a band gap in BLG. Construction of BLG-based van der Waals (vdWs) heterostructures[20,21] and application of strain[22,23] are also predicted to be effective ways to generate a band gap. It has also been reported that the band gap of BLG can be modified by intercalating transition metals between the two graphene layers.[24−26] In addition to using a single approach, band gap opening in BLG by a combination of two approaches, such as molecular doping or uniaxial strain with an external electric field, has been studied theoretically.[27,28] It is found that the resulting band gap in BLG is larger than the gap obtained by either approach alone. Other combinations of approaches are, therefore, likely to provide larger band gaps.

In this paper, we explore band gap opening in BLG that is grown epitaxially on Ru(0001) by intercalating silicon. Intercalated silicon forms a silicene layer with a $\sqrt{7} \times \sqrt{7}$ superstructure with respect to Ru(0001), which is confirmed by low-energy electron diffraction (LEED) and scanning tunneling microscopy (STM). The observed moiré pattern indicates that the BLG is rippled. Raman spectroscopy shows that the underlying silicene effectively decouples the BLG from the Ru substrate and indicates the existence of both doping and strain in the BLG. A sizable band gap of about 0.2 eV is observed in the BLG by angle-resolved photoemission spectroscopy (ARPES). On the basis of density functional theory (DFT) calculations, we conclude that the significant large band gap opening is caused by the cooperative effect of electron doping and rippling.

RESULTS AND DISCUSSION

We fabricated and characterized high-quality BLG on Ru(0001) using the method described in a prior paper[29] (see also Methods). Figure 1a,b shows a schematic to illustrate the process of silicene intercalation between BLG and Ru

Received: January 22, 2020
Revised: February 27, 2020
Published: March 3, 2020

https://dx.doi.org/10.1021/acs.nanolett.0c00306
Nano Lett. 2020, 20, 2674−2680

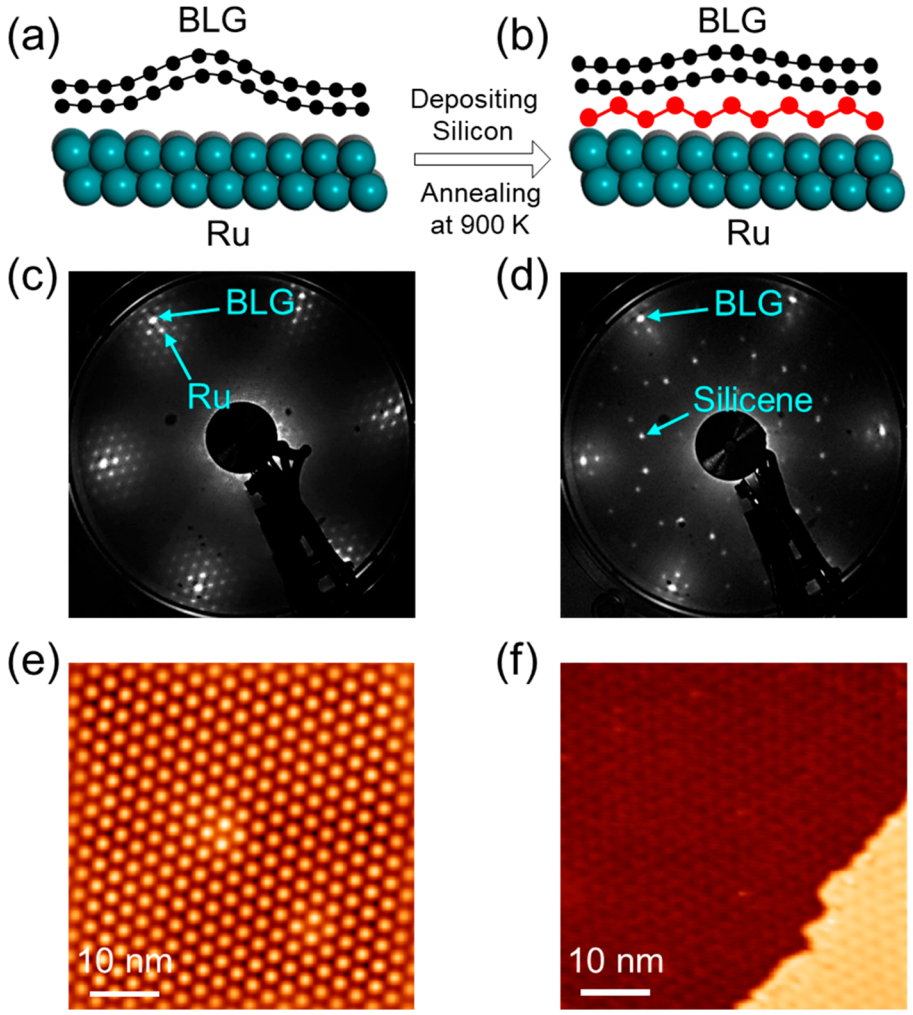

Figure 1. LEED and STM characterizations of BLG on Ru(0001) before and after silicon intercalation. (a,b) Schematic of the process of BLG/silicene heterostructure on Ru(0001). (c,d) LEED patterns (65 eV) of BLG/Ru and BLG/silicene/Ru, respectively. Diffraction spots contributed by BLG, Ru, and silicene are labeled by solid arrows. (e,f) Corresponding STM images for BLG/Ru (V_s = −1 V, I_t = 100 pA) and BLG/silicene/Ru (V_s = −0.5 V, I_t = 400 pA), respectively.

substrate. First, high-quality AB-stacked BLG is epitaxially grown on a clean Ru(0001) surface (Figure 1a). Subsequently, silicon atoms are deposited on the surface of the as-grown BLG followed by annealing to initiate the intercalation. The intercalated silicon atoms form a silicene layer at the interface between the BLG and the Ru substrate (Figure 1b).

To check the results of each step, we performed in situ LEED and STM measurements on the sample. Figure 1c is a LEED pattern of the as-grown BLG on Ru(0001), showing sharp diffraction spots from the BLG and surrounding satellite spots from a moiré pattern. From the STM image, as shown in Figure 1e, we clearly see a defect-free moiré pattern, indicating that the epitaxial graphene is rippled periodically.[30] After depositing silicon followed by the annealing process, the LEED pattern changes significantly. As shown in Figure 1d, diffraction spots from the BLG retain high intensity, whereas the intensity of spots from the moiré pattern weakens. Moreover, a new set of diffraction spots with a $\sqrt{7} \times \sqrt{7}$ superstructure with respect to Ru(0001) emerge. The corresponding STM image is shown in Figure 1f. Compared with Figure 1e, we can see that the periodic moiré superlattice stays intact while the amplitude of surface corrugation decreases. These results suggest that the silicon is intercalated below the BLG, weakening the interaction between BLG and Ru. Note that the existence of a moiré pattern indicates that the BLG is still rippled after silicon intercalation.

To study more detailed local structures, we performed STM measurements across a boundary, as shown in Figure S1a. The apparent height difference across the boundary is about 3.3 Å, as measured by the line profile along the white arrow (Figure S1b). The value is consistent with the interlayer distance of graphite or AB-stacked BLG,[31] indicating a boundary of BLG and single-layer graphene (SLG). Figure S1c,d shows an atomically resolved STM image obtained in the black square in the BLG region and the corresponding fast Fourier transformation (FFT) pattern. We can distinguish the honeycomb lattices of graphene and the underlying silicon superlattices, which are marked by solid and dashed rhombuses, respectively. The silicon superlattice has a periodicity of about 0.72 nm and is rotated 19° relative to Ru(0001). According to previous studies, such $\sqrt{7} \times \sqrt{7}$-R19° superstructure of silicon on a Ru(0001) surface is silicene.[32,33] These results suggest that we realized the intercalation of silicene at the interface between BLG and the Ru substrate.

The effect of the intercalated silicene layer on BLG is examined by Raman characterizations. For comparison, Raman

https://dx.doi.org/10.1021/acs.nanolett.0c00306
Nano Lett. 2020, 20, 2674−2680

spectra of SLG/Ru (black curve), SLG/silicene/Ru (green curve), BLG/Ru (red curve), and BLG/silicene/Ru (blue curve) are shown in Figure 2a. The SLG on Ru exhibits a

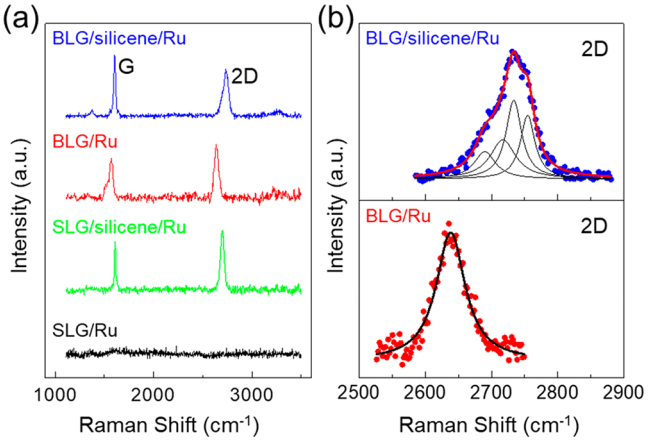

Figure 2. Raman spectra of SLG and BLG on Ru substrate before and after silicene intercalation. (a) Comparison of Raman spectra of SLG/Ru (black), SLG/silicene/Ru (green), BLG/Ru (red), and BLG/silicene/Ru (blue). (b) 2D band of BLG/Ru well fitted by a single narrow Lorentzian peak (lower panel) and 2D band of BLG/silicene/Ru well fitted with four narrow Lorentzian components (upper panel).

featureless Raman spectrum due to strong hybridization between graphene and the Ru substrate.[34] In contrast, after silicene intercalation Raman peaks (G and 2D) appear and the full width at half-maximum (FWHM) of the 2D peak is 32 cm^{-1}, indicative of recovery of intrinsic SLG. The Raman spectrum of BLG on Ru before silicene intercalation shows strong 2D and G peaks with an intensity ratio I_{2D}/I_G of about 1.4. Moreover, as shown in the lower panel of Figure 2b, the 2D band is well fitted by a single Lorentzian peak with FWHM less than 40 cm^{-1}, indicating Raman features of SLG instead of BLG. After silicene intercalation, however, the intensity ratio I_{2D}/I_G reduces to about 0.7, and the 2D band is broadened to 64 cm^{-1} in FWHM and well fitted by four narrow Lorentzian components, as shown in the upper panel of Figure 2b. These results indicate that the epitaxial BLG on Ru recovers its intrinsic properties after silicene intercalation.

Moreover, Raman spectroscopy has been a powerful tool for characterizing doping or ripple/strain in graphene each of which can lead to variations in phonon frequencies.[35−38] On one hand, in the case of BLG, the Raman G band (E_{2g} mode showing strong electron−phonon coupling), which can split into a doublet due to symmetry breaking, is strongly sensitive to doping.[39] The G peak of BLG after silicene intercalation here is broadened (23 cm^{-1} in FWHM) but does not show obvious splitting, indicating that the BLG is slightly doped.[40,41] On the other hand, the 2D peak of BLG is slightly changed at a relatively low doping level according to previous literature.[42] Here, we observe a large blue shift of about 45 cm^{-1} for the 2D peak of the BLG after silicene intercalation compared with freestanding BLG,[43] further confirming the existence of rippling.[44] The amount of strain in graphene ripples can be roughly estimated from the formula $(\Delta\omega_{2D}/\varepsilon) = \omega_0\gamma_{2D}(1 - 0.186)$, $(\partial\omega_{2D}/\partial\varepsilon) = -64$ cm^{-1}%, where ε is the strain, and $\Delta\omega_{2D}$ and γ_{2D} are the shifting and Grüneisen parameters for the 2D peak, respectively.[37,44] We find that the rippling in the BLG/silicene/Ru is ∼0.7% compressive strain in the rippled BLG.

It is reported that intercalation of graphene can not only decouple the interaction between graphene and metal substrates[45−47] but also tune the electronic state of the graphene.[48,49] To investigate the electronic properties of BLG after silicene intercalation, we carried out ARPES measurements. Figure 3a shows the energy-momentum dispersion

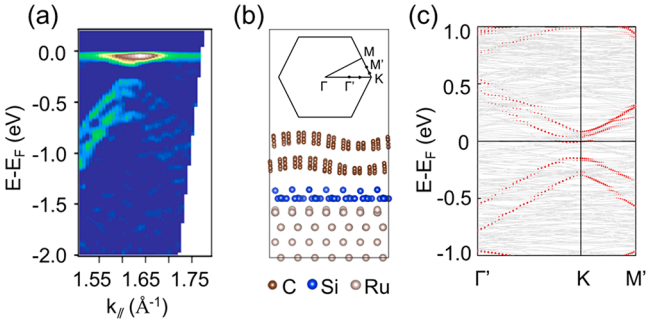

Figure 3. Electronic properties of the BLG after silicene intercalation. (a) ARPES intensity map taken along the Γ-K-M direction. (b) A structure model of rippled BLG on Ru(0001) after silicene intercalation. (c) Calculated band structure based on the structure model in (b). The red dots are the band projected on the BLG and the gray lines are the bands of the whole system.

along the Γ-K-M direction of the Brillouin zone of graphene. The resolved π-band splitting confirms that the sample is AB-stacked BLG.[16,50] We also find that the conduction band minimum is 0.12 eV below the Fermi energy, that is, the BLG is *n*-type doped, which is consistent with the fact that a Ru substrate is known to dope a graphene monolayer.[34,46] This result implies an estimated electron doping of 4.4×10^{12} cm^{-2} in the BLG,[39,51] which agrees with the result of Raman spectroscopy. Most interestingly, by checking the energy distribution curve (EDC) at the K-point (Figure S2), we observe a sizable band gap of 0.20 eV opening in the BLG. These observations provide additional confirmation that we have fabricated BLG on Ru as opposed to SLG on Ru. The latter, after silicon intercalation, shows a linear dispersion without a band gap.[46]

To get a better understanding of the ARPES results, we performed DFT calculations to analyze the electronic properties of BLG with silicene intercalation. On the basis of the experimental observations, the silicene intercalated BLG on Ru (0001) is described by a model with (8×8) BLG sitting on (7×7) 4 layers of ruthenium with $\sqrt{7} \times \sqrt{7}$ silicene between the BLG and ruthenium. As shown in Figure 3b, the BLG is rippled after optimization, which is consistent with the experimental results. We also note that the amplitude of corrugation of the two graphene layers is slightly different, indicating an asymmetric ripple. The band structure of BLG is tuned by the Ru substrate and silicene layer, as shown in Figure 3c. The BLG is n-doped with a band gap of 0.15 eV around the K-point, which is in qualitative agreement with the ARPES results.

We then analyze the mechanism for this sizable band gap opening. From the above analysis, we notice that the electron doping induced by the underlying substrate and asymmetric ripple are two factors affecting the band structure of BLG. We first consider the doping induced by the silicene/Ru substrate on the BLG. To exclude the ripple effect, a structure model

https://dx.doi.org/10.1021/acs.nanolett.0c00306
Nano Lett. 2020, 20, 2674−2680

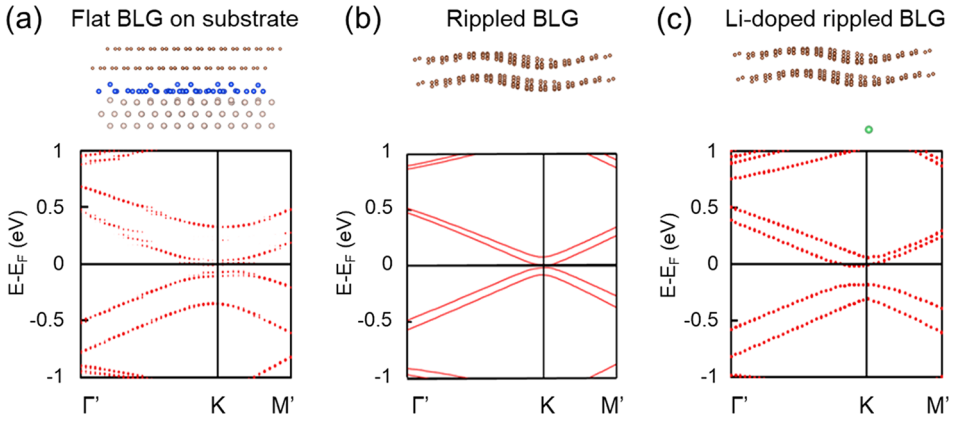

Figure 4. Calculated band structures of the BLG induced by doping and rippling individually. (a) A structure model of flat BLG (3% compressed) on silicene/Ru (upper panel) and calculated band structure (lower panel). (b) A structure model of rippled BLG (upper panel) and calculated band structure based on the model (lower panel). (c) A structure model of Li-doped rippled BLG (upper panel, Li atom (green dot) is put under the rippled BLG) and calculated band structure (lower panel).

with a flat BLG (3% compressed) is placed on the silicene/Ru substrate, as shown in the upper panel of Figure 4a. The calculated band structure in the lower panel of Figure 4a shows a 0.06 eV band gap around the K-point. This result is also supported by the experimental finding that the 4.4×10^{12} cm^{-2} electron doping (derived from ARPES results) should yield a band gap around 0.05 eV.[52] It is also worth noting that the band structures of doped BLG with and without an in-plane 3% compression are identical (see Figure S3). Therefore, we conclude that the band gap induced only by doping is 0.06 eV, which is significantly smaller than the experimentally observed value (0.20 eV) and the calculated value of 0.15 eV.

We subsequently consider the effect of asymmetric rippling of the BLG. The band structure for the rippled BLG with the same atomic configuration as in Figure 3b is calculated. As shown in Figure 4b, the ripple-induced band gap is 0.02 eV, which is also significantly smaller than the experimental result.

As neither the doping nor the rippling alone can induce such a large band gap opening, we consider a cooperative effect of these two factors. Here, for computational efficiency, we use Li atoms to mimic the doping effect of the silicene/Ru substrate as alkali adatoms are known to dope graphene n-type.[16] As shown in Figure 4c, a lithium atom is put under the rippled BLG with a distance of 6.45 Å to generate a doping concentration that is the same as the experimental observation. By considering both rippling and doping, we find that there is a 0.17 eV band gap opening, which is comparable to the experimental value but significantly larger than considering each effect alone. Therefore, we conclude that the doping and asymmetric ripple play a cooperative role in opening a large band gap in BLG.

CONCLUSIONS

In summary, we have investigated the opening of a sizable band gap in an epitaxially grown BLG by a combination of doping and rippling/strain, which are generated by intercalating silicon between a BLG and a Ru substrate. The intercalated silicon forms a silicene layer with a $\sqrt{7} \times \sqrt{7}$ superstructure at the interface between BLG and Ru, which is unambiguously confirmed by LEED and STM characterizations. After silicene intercalation, the Raman features of freestanding BLG are restored, suggesting that the interfacial silicene effectively decouples the BLG from Ru. Large blueshifts of the G and 2D peaks indicate the existence of both doping and rippling in the BLG. ARPES measurements of the electronic structure show a sizable band gap approximately 0.2 eV. DFT calculations reveal that the large band gap is induced by the cooperative interaction of doping and rippling in the BLG.

METHODS

Sample Preparation and Characterizations. The growth of BLG and silicon intercalation were carried out in a home-built ultrahigh vacuum (UHV)-MBE system with a base pressure lower than 2×10^{-9} mbar. First, a Ru(0001) surface was cleaned by repeated cycles of sputtering and annealing treatment. Then, the Ru was exposed to oxygen (5×10^{-7} mbar) at 1070 K for 5 min to remove the residual carbon. High-quality BLG was fabricated by exposing ethylene up to a pressure of 3×10^{-6} mbar at 1420 K for 150 s, followed by cooling down to room temperature at a slow rate of about 60 K min^{-1}.[29] Unlike the annealing temperature of ∼1100 K for growth of SLG,[53,54] here the elevated growth temperature of 1420 K increases carbon solubility in bulk Ru, favoring the growth of uniform and high-quality BLG. Silicon atoms were evaporated to the graphene surface and then annealed at 900 K. STM images were obtained at about 4 K. LEED was employed with a 4-grid detector (Omicron Spectra LEED) in the UHV chamber. Raman spectra were obtained by a commercial confocal Raman microscope (WiTec), using an excitation wavelength of 532 nm. ARPES measurements were carried out using the Scienta R4000 analyzer and VUV5000UV source which gives a photon energy of Helium I at $h\nu$ = 21.218 eV. The energy resolution is better than 30 meV and the angular resolution is 0.3°. The measurement was performed at 30 K in vacuum with a base pressure better than 5×10^{-11} mbar.

DFT Calculations. First-principles calculations were performed using the Vienna Ab Initio Simulation Package (VASP),[55] version 5.4.1, and the projector augmented-wave (PAW) method.[56] Because of computational limitations for the size of our structures, electronic exchange and correlation effects were treated using the local density approximation (LDA).[57] In the calculation, a vacuum layer of 16 Å was used and the energy cutoff of the plane-wave basis set was 500 eV. In the BLG/silicene/Ru model, all atoms except the bottom two Ru layers were relaxed until the net force on every atom is

https://dx.doi.org/10.1021/acs.nanolett.0c00306
Nano Lett. 2020, 20, 2674−2680

smaller than 0.02 eV/Å. The Γ-point was employed for Brillouin zone integrations due to computational limitations. In the Li-doped BLG model, all atoms were relaxed until the net force on every atom is smaller than 0.01 eV/Å and a 6 × 6 *k*-point mesh was used. The LDA method gives an upper limit in evaluating the interactions between graphene and silicene.

■ ASSOCIATED CONTENT

Supporting Information

The Supporting Information is available free of charge at https://pubs.acs.org/doi/10.1021/acs.nanolett.0c00306.

Supporting data, Figures S1−S3. (PDF)

CIF for structure models used in Figure 3, Figure 4, and Figure S3 (ZIP)

■ AUTHOR INFORMATION

Corresponding Authors

Shixuan Du − *Institute of Physics and University of Chinese Academy of Sciences, Chinese Academy of Sciences, Beijing 100190, P.R. China; CAS Center for Excellence in Topological Quantum Computation, University of Chinese Academy of Sciences, Beijing 100190, P.R. China; Songshan Lake Materials Laboratory, Dongguan, Guangdong 523808, P.R. China;* orcid.org/0000-0001-9323-1307; Email: sxdu@iphy.ac.cn

Hong-Jun Gao − *Institute of Physics and University of Chinese Academy of Sciences, Chinese Academy of Sciences, Beijing 100190, P.R. China; CAS Center for Excellence in Topological Quantum Computation, University of Chinese Academy of Sciences, Beijing 100190, P.R. China; Songshan Lake Materials Laboratory, Dongguan, Guangdong 523808, P.R. China;* Email: hjgao@iphy.ac.cn

Authors

Hui Guo − *Institute of Physics and University of Chinese Academy of Sciences, Chinese Academy of Sciences, Beijing 100190, P.R. China*

Ruizi Zhang − *Institute of Physics and University of Chinese Academy of Sciences, Chinese Academy of Sciences, Beijing 100190, P.R. China*

Hang Li − *Institute of Physics and University of Chinese Academy of Sciences, Chinese Academy of Sciences, Beijing 100190, P.R. China*

Xueyan Wang − *Institute of Physics and University of Chinese Academy of Sciences, Chinese Academy of Sciences, Beijing 100190, P.R. China*

Hongliang Lu − *Institute of Physics and University of Chinese Academy of Sciences, Chinese Academy of Sciences, Beijing 100190, P.R. China; CAS Center for Excellence in Topological Quantum Computation, University of Chinese Academy of Sciences, Beijing 100190, P.R. China*

Kai Qian − *Institute of Physics and University of Chinese Academy of Sciences, Chinese Academy of Sciences, Beijing 100190, P.R. China*

Geng Li − *Institute of Physics and University of Chinese Academy of Sciences, Chinese Academy of Sciences, Beijing 100190, P.R. China;* orcid.org/0000-0002-3347-7222

Li Huang − *Institute of Physics and University of Chinese Academy of Sciences, Chinese Academy of Sciences, Beijing 100190, P.R. China*

Xiao Lin − *Institute of Physics and University of Chinese Academy of Sciences, Chinese Academy of Sciences, Beijing 100190, P.R. China; CAS Center for Excellence in Topological Quantum Computation, University of Chinese Academy of Sciences, Beijing 100190, P.R. China*

Yu-Yang Zhang − *Institute of Physics and University of Chinese Academy of Sciences, Chinese Academy of Sciences, Beijing 100190, P.R. China; CAS Center for Excellence in Topological Quantum Computation, University of Chinese Academy of Sciences, Beijing 100190, P.R. China;* orcid.org/0000-0002-9548-0021

Hong Ding − *Institute of Physics and University of Chinese Academy of Sciences, Chinese Academy of Sciences, Beijing 100190, P.R. China; CAS Center for Excellence in Topological Quantum Computation, University of Chinese Academy of Sciences, Beijing 100190, P.R. China; Songshan Lake Materials Laboratory, Dongguan, Guangdong 523808, P.R. China*

Sokrates T. Pantelides − *Institute of Physics and University of Chinese Academy of Sciences, Chinese Academy of Sciences, Beijing 100190, P.R. China; Department of Physics and Astronomy and Department of Electrical Engineering and Computer Science, Vanderbilt University, Nashville, Tennessee 37235, United States;* orcid.org/0000-0002-2963-7545

Complete contact information is available at: https://pubs.acs.org/10.1021/acs.nanolett.0c00306

Author Contributions

The manuscript was written through contributions of all authors. All authors have given approval to the final version of the manuscript.

Author Contributions

⊥H.G., R.Z.Z., and H.L. contributed equally to this work.

Notes

The authors declare no competing financial interest.

■ ACKNOWLEDGMENTS

We acknowledge the grants from National Key Research & Development Projects of China (Nos. 2016YFA0202300, 2018YFA0305800, and 2019YFA0308500), National Natural Science Foundation of China (Nos. 61888102, 51872284, and 51922011), the Strategic Priority Research Program of Chinese Academy of Sciences (Nos. XDB30000000, XDB28000000), Beijing Nova Program (No. Z181100006218023), the CAS Pioneer Hundred Talents Program, and the K. C. Wong Education. Work at Vanderbilt (S.T.P.) was supported by the McMinn Endowment. Computational resources were provided by the National Supercomputing Center in Tianjin. A portion of the research was performed in CAS Key Laboratory of Vacuum Physics.

■ REFERENCES

(1) Rozhkov, A. V.; Sboychakov, A. O.; Rakhmanov, A. L.; Nori, F. Electronic properties of graphene-based bilayer systems. *Phys. Rep.* **2016**, *648*, 1−104.

(2) McCann, E.; Koshino, M. The electronic properties of bilayer graphene. *Rep. Prog. Phys.* **2013**, *76*, No. 056503.

(3) Park, C. H.; Louie, S. G. Tunable excitons in biased bilayer graphene. *Nano Lett.* **2010**, *10*, 426−431.

(4) Ju, L.; Wang, L.; Cao, T.; Taniguchi, T.; Watanabe, K.; Louie, S. G.; Rana, F.; Park, J.; Hone, J.; Wang, F.; McEuen, P. L. Tunable excitons in bilayer graphene. *Science* **2017**, *358*, 907−910.

(5) Sui, M. Q.; Chen, G. R.; Ma, L. G.; Shan, W. Y.; Tian, D.; Watanabe, K.; Taniguchi, T.; Jin, X. F.; Yao, W.; Xiao, D.; Zhang, Y. B. Gate-tunable topological valley transport in bilayer graphene. *Nat. Phys.* **2015**, *11*, 1027−1032.

(6) Cao, Y.; Fatemi, V.; Demir, A.; Fang, S.; Tomarken, S. L.; Luo, J. Y.; Sanchez-Yamagishi, J. D.; Watanabe, K.; Taniguchi, T.; Kaxiras, E.; Ashoori, R. C.; Jarillo-Herrero, P. Correlated insulator behaviour at half-filling in magic-angle graphene superlattices. *Nature* **2018**, *556*, 80−84.
(7) Cao, Y.; Fatemi, V.; Fang, S.; Watanabe, K.; Taniguchi, T.; Kaxiras, E.; Jarillo-Herrero, P. Unconventional superconductivity in magic-angle graphene superlattices. *Nature* **2018**, *556*, 43−50.
(8) Lee, S. Y.; Duong, D. L.; Vu, Q. A.; Jin, Y.; Kim, P.; Lee, Y. H. Chemically modulated band gap in bilayer graphene memory transistors with high on/off ratio. *ACS Nano* **2015**, *9*, 9034−9042.
(9) Yan, J.; Kim, M. H.; Elle, J. A.; Sushkov, A. B.; Jenkins, G. S.; Milchberg, H. M.; Fuhrer, M. S.; Drew, H. D. Dual-gated bilayer graphene hot-electron bolometer. *Nat. Nanotechnol.* **2012**, *7*, 472−478.
(10) Xia, F. N.; Farmer, D. B.; Lin, Y. M.; Avouris, P. Graphene field-effect transistors with high on/off current ratio and large transport band gap at room temperature. *Nano Lett.* **2010**, *10*, 715−718.
(11) Castro, E. V.; Novoselov, K. S.; Morozov, S. V.; Peres, N. M. R.; Dos Santos, J. M. B. L.; Nilsson, J.; Guinea, F.; Geim, A. K.; Castro Neto, A. H. Biased bilayer graphene: Semiconductor with a gap tunable by the electric field effect. *Phys. Rev. Lett.* **2007**, *99*, 216802.
(12) Zhang, Y. B.; Tang, T. T.; Girit, C.; Hao, Z.; Martin, M. C.; Zettl, A.; Crommie, M. F.; Shen, Y. R.; Wang, F. Direct observation of a widely tunable bandgap in bilayer graphene. *Nature* **2009**, *459*, 820−823.
(13) Oostinga, J. B.; Heersche, H. B.; Liu, X. L.; Morpurgo, A. F.; Vandersypen, L. M. K. Gate-induced insulating state in bilayer graphene devices. *Nat. Mater.* **2008**, *7*, 151−157.
(14) Mak, K. F.; Lui, C. H.; Shan, J.; Heinz, T. F. Observation of an electric-field-induced band gap in bilayer graphene by infrared spectroscopy. *Phys. Rev. Lett.* **2009**, *102*, 256405.
(15) Denis, P. A. Band gap opening of monolayer and bilayer graphene doped with aluminium, silicon, phosphorus, and sulfur. *Chem. Phys. Lett.* **2010**, *492*, 251−257.
(16) Ohta, T.; Bostwick, A.; Seyller, T.; Horn, K.; Rotenberg, E. Controlling the electronic structure of bilayer graphene. *Science* **2006**, *313*, 951−954.
(17) Samuels, A. J.; Carey, J. D. Molecular doping and band-gap opening of bilayer graphene. *ACS Nano* **2013**, *7*, 2790−2799.
(18) Zhang, W. J.; Lin, C. T.; Liu, K. K.; Tite, T.; Su, C. Y.; Chang, C. H.; Lee, Y. H.; Chu, C. W.; Wei, K. H.; Kuo, J. L.; Li, L. J. Opening an electrical band gap of bilayer graphene with molecular doping. *ACS Nano* **2011**, *5*, 7517−7524.
(19) Yu, W. J.; Liao, L.; Chae, S. H.; Lee, Y. H.; Duan, X. F. Toward tunable band gap and tunable dirac point in bilayer graphene with molecular doping. *Nano Lett.* **2011**, *11*, 4759−4763.
(20) Tang, S. B.; Wu, W. H.; Xie, X. J.; Li, X. K.; Gu, J. J. Band gap opening of bilayer graphene by graphene oxide support doping. *RSC Adv.* **2017**, *7*, 9862−9871.
(21) Hao, J. L.; Huang, C. X.; Wu, H. P.; Qiu, Y. H.; Gao, Q.; Hu, Z. P.; Kan, E.; Zhang, L. X. A promising way to open an energy gap in bilayer graphene. *Nanoscale* **2015**, *7*, 17096−17101.
(22) Choi, S. M.; Jhi, S. H.; Son, Y. W. Controlling energy gap of bilayer graphene by strain. *Nano Lett.* **2010**, *10*, 3486−3489.
(23) Verberck, B.; Partoens, B.; Peeters, F. M.; Trauzettel, B. Strain-induced band gaps in bilayer graphene. *Phys. Rev. B: Condens. Matter Mater. Phys.* **2012**, *85*, 125403.
(24) Pakhira, S.; Mendoza-Cortes, J. L. Tuning the Dirac cone of bilayer and bulk structure graphene by intercalating first row transition metals using first-principles calculations. *J. Phys. Chem. C* **2018**, *122*, 4768−4782.
(25) Pakhira, S.; Lucht, K. P.; Mendoza-Cortes, J. L. Dirac cone in two dimensional bilayer graphene by intercalation with V, Nb, and Ta transition metals. *J. Chem. Phys.* **2018**, *148*, No. 064707.
(26) Hui, J.; Pakhira, S.; Bhargava, R.; Barton, Z. J.; Zhou, X.; Chinderle, A. J.; Mendoza-Cortes, J. L.; Rodríguez-López, J. Modulating electrocatalysis on graphene heterostructures: physically impermeable yet electrobically transparent electrodes. *ACS Nano* **2018**, *12*, 2980−2990.
(27) Tian, X. Q.; Xu, J. B.; Wang, X. M. Band gap opening of bilayer graphene by F4-TCNQ molecular doping and externally applied electric field. *J. Phys. Chem. B* **2010**, *114*, 11377−11381.
(28) Nanda, B. R. K.; Satpathy, S. Strain and electric field modulation of the electronic structure of bilayer graphene. *Phys. Rev. B: Condens. Matter Mater. Phys.* **2009**, *80*, 165430.
(29) Guo, H.; Wang, X.; Lu, H.; Bao, L.; Peng, H.; Qian, K.; Ma, J.; Li, G.; Huang, L.; Lin, X.; Zhang, Y.-Y.; Du, S.; Pantelides, S. T.; Gao, H.-J. Centimeter-scale, single-crystalline, AB-stacked bilayer graphene on insulating substrates. *2D Mater.* **2019**, *6*, No. 045044.
(30) de Parga, A. L. V.; Calleja, F.; Borca, B.; Passeggi, M. C. G.; Hinarejos, J. J.; Guinea, F.; Miranda, R. Periodically rippled graphene: growth and spatially resolved electronic structure. *Phys. Rev. Lett.* **2008**, *100*, No. 056807.
(31) Lee, J. K.; Kim, J. G.; Hembram, K. P. S. S.; Kim, Y. I.; Min, B. K.; Park, Y.; Lee, J. K.; Moon, D. J.; Lee, W.; Lee, S. G.; John, P. The Nature of metastable AA' graphite: low dimensional nano- and single-crystalline forms. *Sci. Rep.* **2016**, *6*, 39624.
(32) Huang, L.; Zhang, Y. F.; Zhang, Y. Y.; Xu, W. Y.; Que, Y. D.; Li, E.; Pan, J. B.; Wang, Y. L.; Liu, Y. Q.; Du, S. X.; Pantelides, S. T.; Gao, H.-J. Sequence of silicon monolayer structures grown on a Ru surface: from a Herringbone structure to silicene. *Nano Lett.* **2017**, *17*, 1161−1166.
(33) Li, G.; Zhang, L. Z.; Xu, W. Y.; Pan, J. B.; Song, S. R.; Zhang, Y.; Zhou, H. T.; Wang, Y. L.; Bao, L. H.; Zhang, Y.-Y.; Du, S. X.; Ouyang, M.; Pantelides, S. T.; Gao, H.-J. Stable silicene in graphene/silicene van der Waals heterostructures. *Adv. Mater.* **2018**, *30*, 1804650.
(34) Sutter, P.; Hybertsen, M. S.; Sadowski, J. T.; Sutter, E. Electronic structure of few-layer epitaxial graphene on Ru(0001). *Nano Lett.* **2009**, *9*, 2654−2660.
(35) Lee, J. E.; Ahn, G.; Shim, J.; Lee, Y. S.; Ryu, S. Optical separation of mechanical strain from charge doping in graphene. *Nat. Commun.* **2012**, *3*, 1024.
(36) Das, A.; Pisana, S.; Chakraborty, B.; Piscanec, S.; Saha, S. K.; Waghmare, U. V.; Novoselov, K. S.; Krishnamurthy, H. R.; Geim, A. K.; Ferrari, A. C.; Sood, A. K. Monitoring dopants by Raman scattering in an electrochemically top-gated graphene transistor. *Nat. Nanotechnol.* **2008**, *3*, 210−215.
(37) Mohiuddin, T. M. G.; Lombardo, A.; Nair, R. R.; Bonetti, A.; Savini, G.; Jalil, R.; Bonini, N.; Basko, D. M.; Galiotis, C.; Marzari, N.; Novoselov, K. S.; Geim, A. K.; Ferrari, A. C. Uniaxial strain in graphene by Raman spectroscopy: G peak splitting, Grüneisen parameters, and sample orientation. *Phys. Rev. B: Condens. Matter Mater. Phys.* **2009**, *79*, 205433.
(38) Ferrari, A. C.; Basko, D. M. Raman spectroscopy as a versatile tool for studying the properties of graphene. *Nat. Nanotechnol.* **2013**, *8*, 235−246.
(39) Malard, L. M.; Elias, D. C.; Alves, E. S.; Pimenta, M. A. Observation of distinct electron-phonon couplings in gated bilayer graphene. *Phys. Rev. Lett.* **2008**, *101*, 257401.
(40) Mafra, D. L.; Gava, P.; Malard, L. M.; Borges, R. S.; Silva, G. G.; Leon, J. A.; Plentz, F.; Mauri, F.; Pimenta, M. A. Characterizing intrinsic charges in top gated bilayer graphene device by Raman spectroscopy. *Carbon* **2012**, *50*, 3435−3439.
(41) Yan, J.; Villarson, T.; Henriksen, E. A.; Kim, P.; Pinczuk, A. Optical phonon mixing in bilayer graphene with a broken inversion symmetry. *Phys. Rev. B: Condens. Matter Mater. Phys.* **2009**, *80*, 241417.
(42) Das, A.; Chakraborty, B.; Piscanec, S.; Pisana, S.; Sood, A. K.; Ferrari, A. C. Phonon renormalization in doped bilayer graphene. *Phys. Rev. B: Condens. Matter Mater. Phys.* **2009**, *79*, 155417.
(43) Malard, L. M.; Nilsson, J.; Elias, D. C.; Brant, J. C.; Plentz, F.; Alves, E. S.; Castro Neto, A. H.; Pimenta, M. A. Probing the electronic structure of bilayer graphene by Raman scattering. *Phys. Rev. B: Condens. Matter Mater. Phys.* **2007**, *76*, 201401.

https://dx.doi.org/10.1021/acs.nanolett.0c00306
Nano Lett. 2020, 20, 2674−2680

(44) Wang, Y.; Yang, R.; Shi, Z. W.; Zhang, L. C.; Shi, D. X.; Wang, E.; Zhang, G. Y. Super-elastic graphene ripples for flexible strain sensors. *ACS Nano* **2011**, *5*, 3645−3650.
(45) Guo, H.; Wang, X.; Bao, D.-L.; Lu, H.-L.; Zhang, Y.-Y.; Li, G.; Wang, Y.-L.; Du, S.-X.; Gao, H.-J. Fabrication of large-scale graphene/2D-germanium heterostructure by intercalation. *Chin. Phys. B* **2019**, *28*, No. 078103.
(46) Mao, J. H.; Huang, L.; Pan, Y.; Gao, M.; He, J. F.; Zhou, H. T.; Guo, H. M.; Tian, Y.; Zou, Q.; Zhang, L. Z.; Zhang, H. G.; Wang, Y. L.; Du, S. X.; Zhou, X. J.; Neto, A. H. C.; Gao, H. J. Silicon layer intercalation of centimeter-scale, epitaxially grown monolayer graphene on Ru(0001). *Appl. Phys. Lett.* **2012**, *100*, No. 093101.
(47) Chen, H.; Que, Y.; Tao, L.; Zhang, Y.-Y.; Lin, X.; Xiao, W.; Wang, D.; Du, S.; Pantelides, S. T.; Gao, H.-J. Recovery of edge states of graphene nanoislands on an iridium substrate by silicon intercalation. *Nano Res.* **2018**, *11*, 3722−3729.
(48) Gao, Y. X.; Zhang, Y. Y.; Du, S. X. Recovery of the Dirac states of graphene by intercalating two-dimensional traditional semiconductors. *J. Phys.: Condens. Matter* **2019**, *31*, 194001.
(49) Schulzendorf, M.; Hinaut, A.; Kisiel, M.; Jöhr, R.; Pawlak, R.; Restuccia, P.; Meyer, E.; Righi, M. C.; Glatzel, T. Altering the properties of graphene on Cu(111) by intercalation of potassium bromide. *ACS Nano* **2019**, *13*, 5485−5492.
(50) Castro Neto, A. H.; Guinea, F.; Peres, N. M. R.; Novoselov, K. S.; Geim, A. K. The electronic properties of graphene. *Rev. Mod. Phys.* **2009**, *81*, 109−162.
(51) Ando, T. Anomaly of optical phonons in bilayer graphene. *J. Phys. Soc. Jpn.* **2007**, *76*, 104711.
(52) McCann, E. Asymmetry gap in the electronic band structure of bilayer graphene. *Phys. Rev. B: Condens. Matter Mater. Phys.* **2006**, *74*, 161403.
(53) Pan, Y.; Shi, D. X.; Gao, H.-J. Formation of graphene on Ru(0001) surface. *Chin. Phys.* **2007**, *16*, 3151−3153.
(54) Pan, Y.; Zhang, H. G.; Shi, D. X.; Sun, J. T.; Du, S. X.; Liu, F.; Gao, H.-J. Highly ordered, millimeter-scale, continuous, single-crystalline graphene monolayer formed on Ru(0001). *Adv. Mater.* **2009**, *21*, 2777−2780.
(55) Kresse, G.; Furthmüller, J. Efficient iterative schemes for ab initio total-energy calculations using a plane-wave basis set. *Phys. Rev. B: Condens. Matter Mater. Phys.* **1996**, *54*, 11169−11186.
(56) Blöchl, P. E. Projector augmented-wave method. *Phys. Rev. B: Condens. Matter Mater. Phys.* **1994**, *50*, 17953−17979.
(57) Perdew, J. P.; Zunger, A. Self-interaction correction to density-functional approximations for many-electron systems. *Phys. Rev. B: Condens. Matter Mater. Phys.* **1981**, *23*, 5048−5079.

https://dx.doi.org/10.1021/acs.nanolett.0c00306
Nano Lett. 2020, 20, 2674−2680